

Accessing non-natural reactivity by irradiating nicotinamide-dependent enzymes with light

Megan A. Emmanuel, Norman R. Greenberg, Daniel G. Oblinsky & Todd K. Hyster

Enzymes are ideal for use in asymmetric catalysis by the chemical industry, because their chemical compositions can be tailored to a specific substrate and selectivity pattern while providing efficiencies and selectivities that surpass those of classical synthetic methods¹. However, enzymes are limited to reactions that are found in nature and, as such, facilitate fewer types of transformation than do other forms of catalysis². Thus, a longstanding challenge in the field of biologically mediated catalysis has been to develop enzymes with new catalytic functions³. Here we describe a method for achieving catalytic promiscuity that uses the photoexcited state of nicotinamide co-factors (molecules that assist enzyme-mediated catalysis). Under irradiation with visible light, the nicotinamide-dependent enzyme known as ketoreductase can be transformed from a carbonyl reductase into an initiator of radical species and a chiral source of hydrogen atoms. We demonstrate this new reactivity through a highly enantioselective radical dehalogenation of lactones—a challenging transformation for small-molecule catalysts^{4–7}. Mechanistic experiments support the theory that a radical species acts as an intermediate in this reaction, with NADH and NADPH (the reduced forms of nicotinamide adenine nucleotide and nicotinamide adenine dinucleotide phosphate, respectively) serving as both a photoreductant and the source of hydrogen atoms. To our knowledge, this method represents the first example of photo-induced enzyme promiscuity, and highlights the potential for accessing new reactivity from existing enzymes simply by using the excited states of common biological co-factors. This represents a departure from existing light-driven biocatalytic techniques, which are typically explored in the context of co-factor regeneration^{8,9}.

Living organisms use photoactive co-factors to convert light into chemical energy, driving a litany of biologically essential enzymatic reactions. In these systems, the small-molecule co-factor collects solar energy, while the structure of the associated enzyme dictates how the energy is converted into chemical reactivity. Such specialization of function enables diverse reactivity to be achieved with a small number of photoactive co-factors. Flavin, for example, contributes to the repair of thiamine dimers by one enzyme, the induction of flagellum-mediated locomotion by another, and the setting of circadian rhythms by yet another¹⁰. Yet despite this diversity of function, light-responsive enzymes that act on small organic molecules—generating useful radical species that could drive subsequent reactivity—are rare¹¹. In contrast, in synthetic photoredox catalysis, photon-responsive molecules are commonly used to generate organic radicals from small organic molecules¹². We hypothesized that if enzymes with photoactive co-factors could be adapted to generate radical intermediates, it might be possible to catalyse asymmetric radical-driven reactions.

In designing our system, we sought proteins in which the binding site for organic substrates is adjacent to the binding site for a photoreponsive co-factor, with the expectation that substrate binding might therefore elicit superior selectivity for radical transformations¹³. As regards the co-factor, we were interested in NADH/NADPH, owing to their unique photophysical properties. In its ground state, NADH

(or NADPH) is primarily understood as a hydride (H^-) source and a weak single-electron reductant. But upon photoexcitation it becomes a potent single-electron reductant that can reduce an array of functional groups (Fig. 1a)^{14–17}. For example, the calculated oxidation potential of photoexcited 1-benzyl-1,4-dihydronicotinamide (BNAH⁺, an NADH model) for a saturated calomel electrode, a standard reference electrode, is -2.6 V; BNAH⁺ also has a low homolytic bond-dissociation free energy (the energy required to break a covalently bonded molecule into two radicals) for the C4–H bond (this energy requirement is 32 kcal mol⁻¹ for acetonitrile), thus enabling a thermodynamically favourable transfer of hydrogen atoms (H^\bullet) to most radical species¹⁸.

In our model system, we tested nicotinamide-dependent ketoreductases (KREDs) for their ability to act as an initiator of radical species and a chiral hydrogen-atom source for radical dehalogenation reactions (Fig. 1b)^{19,20}. KREDs are widely used in the production of chemicals, reducing ketones to enantiomerically pure alcohols via hydride transfer (Fig. 1c)²¹. The ubiquity, utility and evolvability of KREDs have made them essential tools in chemical synthesis and, as such, panels of structurally diverse KREDs are commercially available.

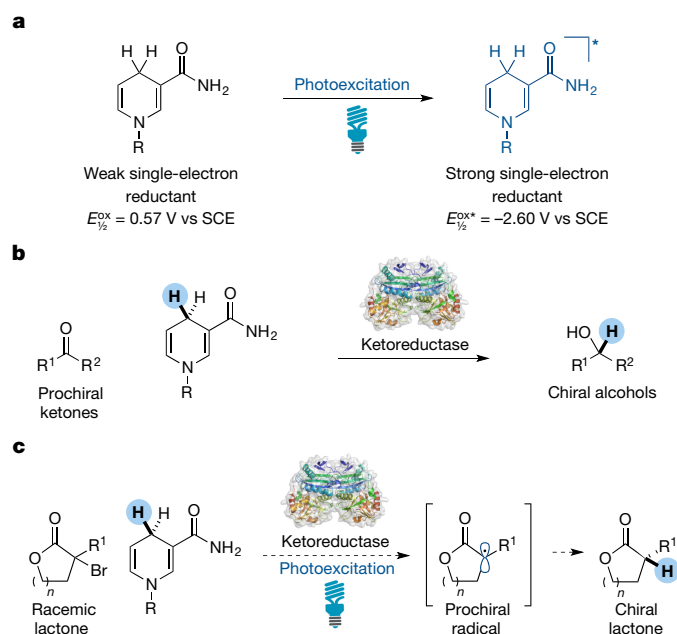
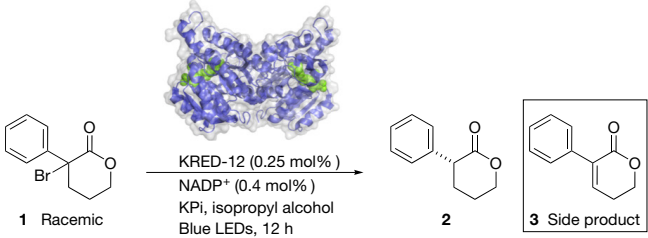


Figure 1 | Photon-induced promiscuity in a biocatalytic process. **a**, Ground-state nicotinamide (left) is understood to serve as a hydride (H^-) source and is a weak single-electron reductant. However, when excited (right), it becomes a potent single-electron reductant. $E_{1/2}^{ox}$, oxidation potential; R, organic functional group; SCE, saturated calomel electrode. **b**, Ketoreductases (KREDs) are highly selective enzymes that catalyse the delivery of hydride from NAD(P)H to prochiral ketones, to access chiral alcohols. **c**, Photoexciting NAD(P)H that is bound to the active site of a KRED should allow for the conversion of racemic halolactones to chiral lactones through an intermediate prochiral radical.

Table 1 | Reaction optimization and control experiments


Entry*	Variations from standard conditions	e.r.	Yield (%)
1	None	98/2	81
2 [†]	Purified enzyme	98/2	85
3	No enzyme	—	<1
4	No light	—	<1
5 [‡]	No NADP ⁺	—	<1
6 [‡]	GDH instead of KRED	—	<1
7 [‡]	LKADH (5 mol%)	—	<1
8 [‡]	LKADH-Y190C (5 mol%)	—	3
9 [‡]	LKADH-E145F-F147L-Y190C (5 mol%)	96/4	72
10 [‡]	SYADH (1 mol%)	37/63	5
11 ^{††}	RasADH (1 mol%)	7.5/92.5	51

Y190C refers to a mutation of the tyrosine amino acid at position 190 in LKADH to cysteine. E145F, glutamic acid 145 is mutated to phenylalanine. F147L, phenylalanine 147 is mutated to leucine.

*The diagram shows the standard reaction, which was performed at 0.038 mmol scale in 1.25 ml of buffer (made with 1,000 μ l of 125 mM potassium phosphate buffer (KPi) at pH 6.5; 200 μ l isopropyl alcohol; 50 μ l dimethylsulfoxide (DMSO)). Yields were determined by high-performance liquid chromatography (HPLC) relative to an internal standard. Enantioselectivities were determined by chiral HPLC.

[†]Determined using purified protein.

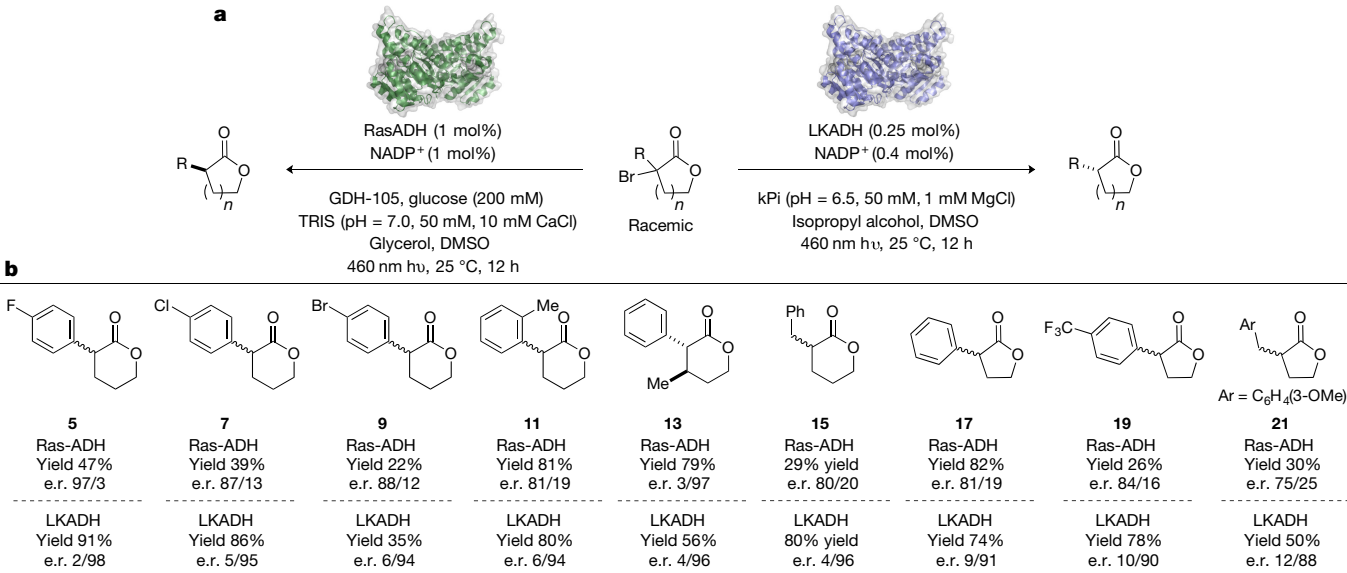
[‡]KRED was replaced with glucose dehydrogenase (GDH).

^{††}Reaction was performed at 0.03 mmol scale in 1.05 ml of buffer (comprising 1,000 μ l of 100 mM TRIS at pH 7.0; 10 mM CaCl₂; 10% glycerol; 200 mM glucose; 50 μ l DMSO) with 5 mg GDH-105.

We selected halogenated lactones as model substrates because they can bind to the active sites of KREDs without being susceptible to carbonyl reduction²².

We tested the viability of the proposed dehalogenation by using a panel of KREDs purchased from Codexis. A halolactone (compound **1**) was reacted with a KRED (0.25 mol%) and NADP⁺ (0.4 mol%) in a 20/4/1 mixture of phosphate buffer (125 mM, pH 6.5 with 2 mM MgSO₄)/isopropyl alcohol/dimethylsulfoxide, and then irradiated with blue LEDs (460 nm). Under these conditions, ten KREDs were ineffective, another seven provided the desired lactone (compound **2**) at modest yield and variable enantioselectivity, and three variants (KRED-4, KRED-12 and KRED-14) provided lactone **2** with a conversion rate of greater than 95%, a yield of 81%, and an enantiomeric ratio (e.r.) of 98/2 in favour of the (*R*)-enantiomer, with dehydrolactone (compound **3**) as the major side product (Table 1, entries 1, 2, and Extended Data Table 1). In suboptimal reactions, the mass balance comprises largely unreacted starting material, with variable amounts of dehydrolactone (**3**). Notably, compound **3** was completely unreactive under the reaction conditions, eliminating the possibility of a selective alkene reduction (Extended Data Figs 1, 2).

We carried out control experiments in order to elucidate the requirements for this reaction. In the absence of KRED, NADP⁺ or light, we detected unreacted starting material and trace amounts of elimination product (Table 1, entries 3–5). Surprisingly, increasing the concentration of NADP⁺ from 0.4 mol% to 50 mol% produced only a modest decrease in enantioselectivity (Extended Data Fig. 3). Furthermore, when a KRED was replaced with glucose dehydrogenase—in order to turn over NADP⁺ without providing an active site for substrate binding—trace amounts of product were observed (Table 1, entry 6). These results suggest that NADPH that is not bound to an enzyme is far less reactive than bound NADPH. To test this hypothesis, we determined the fluorescence lifetime of NADPH with and without protein: in solution, this lifetime is 0.405 ns; in the protein, the lifetime increases more than 20-fold to 9.00 ns (Extended Data Fig. 5 and Extended Data Table 2)²³. The results of ultraviolet/visible-light experiments suggest that a charge-transfer complex is formed between halolactone (**1**) and NADPH only in the presence of KRED (Extended Data Fig. 4). It is likely that this complex is responsible for the initial electron transfer. These experiments support the hypothesis



Entry	Enzyme	Yield	e.r.
5	Ras-ADH	47%	97/3
7	Ras-ADH	39%	87/13
9	Ras-ADH	22%	88/12
11	Ras-ADH	81%	81/19
13	Ras-ADH	79%	3/97
15	Ras-ADH	29% yield	80/20
17	Ras-ADH	82%	81/19
19	Ras-ADH	26%	84/16
21	Ras-ADH	30%	75/25
5	LKADH	91%	2/98
7	LKADH	86%	5/95
9	LKADH	35%	6/94
11	LKADH	80%	6/94
13	LKADH	56%	4/96
15	LKADH	80% yield	4/96
17	LKADH	74%	9/91
19	LKADH	78%	10/90
21	LKADH	50%	12/88

Figure 2 | Substrate scope. An array of different halolactones is amenable to selective dehalogenation activity, providing the (*R*)-enantiomer when using an LKADH variant, or the (*S*)-enantiomer when using RasADH.

a, The basic reactions, starting with a racemic halolactone (centre) and using RasADH (left) or LKADH (right) to catalyse the reactions. The reaction conditions were as follows. For RasADH: halolactone (1 equiv, 40 mM), enzyme (1 mol%), GDH-105 (5 mg), NADP⁺ (1 mol%), glucose (250 mM), TRIS buffer (pH = 7.0, 50 mM, 1 mM CaCl₂, 10% glycerol, 5% dimethylsulfoxide (DMSO), 460 nm, 25 °C, 12 h. For LKADH: halolactone

(1 equiv, 40 mM), enzyme (KRED-12, 0.25 mol%), NADP⁺ (0.25 mol%), KPi buffer (pH = 7.0, 50 mM, 1 mM MgCl₂, 20% isopropyl alcohol, 5% DMSO), 450 nm, 25 °C, 12 h. **b**, The different halolactones that were used as starting points, along with the yields and enantiomeric ratios (e.r.) of the products. For halolactone **13**, isotopic labelling suggests that the product rapidly epimerized to the thermodynamically favourable *trans*-product (Supplementary Fig. 9). For halolactones **14**, **16**, **18** and **20**, in the LKADH experiment, KRED-3 was used instead of KRED-12.

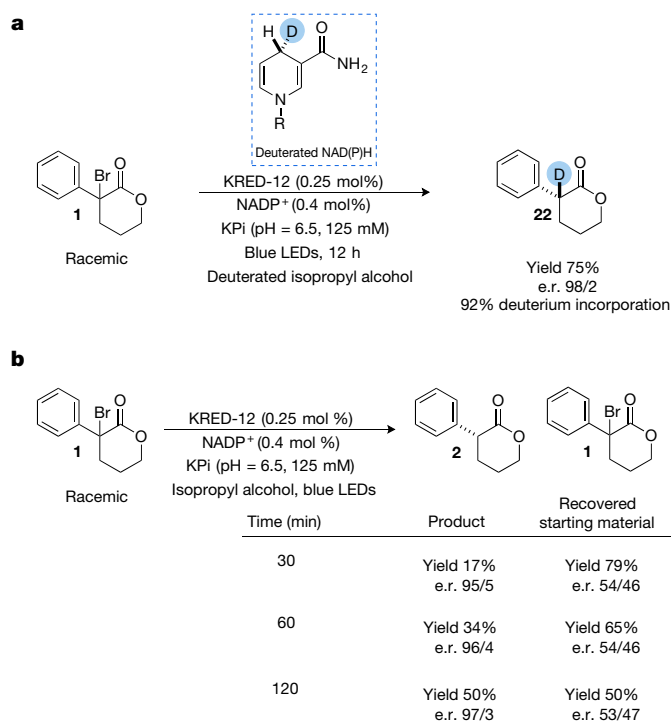
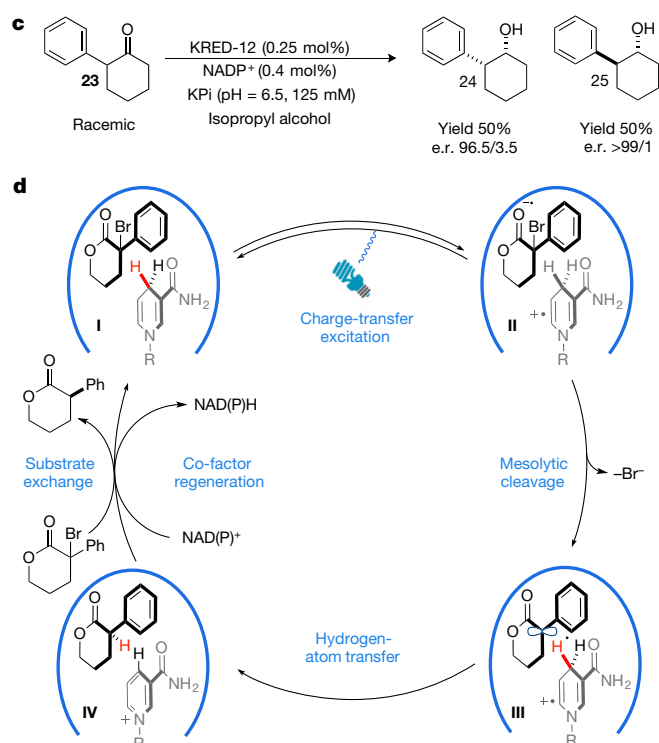


Figure 3 | Mechanistic experiments. **a**, After generating deuterated (D) NAD(P)H *in situ* from deuterated isopropyl alcohol, and under KRED-mediated catalysis, the predominant product is deuterolactone (**22**), showing that NAD(P)H is the hydrogen-atom source in the reaction. **b**, At the end of each reaction, neither enantiomer of starting material is recovered in preference to the other, suggesting that neither enantiomer is preferred by the enzyme. **c**, The most reactive variant of KRED-12 is reactive on both enantiomers of structurally related ketone **23**, supporting the idea that KRED-12 can effect reactions on bulky substrates. **d**, In our proposed mechanism for enantioselective radical dehalogenation, the charge-transfer complex (I) comprises either enantiomer of halolactone



(bold) plus NAD(P)H (grey) within the active site of KRED (blue curve). Photoexcitation effects an electron transfer to form complex II, in which the halolactone and NAD(P)H are both radicals (denoted by \cdot). Upon mesolytic cleavage of the C–Br bond (that is, dehalogenation), complex III is formed, in which the halolactone is a prochiral radical. Then, a conformational change within the enzyme's active site enables hydrogen-atom transfer to the lactone to form an enantioselective product within complex IV. Finally, NAD(P) $^+$ can be reduced by either isopropyl alcohol (using native alcohol dehydrogenase activity) or glucose dehydrogenase to complete the catalytic cycle.

that NADPH is stabilized by the protein and increases the quantum yield of the reaction, providing a possible rationale for the negligible racemic background reaction.

Building on the results obtained with the commercially available kit, we explored the potential of structurally characterized KREDs to effect this transformation. Personal correspondence with G. Huisman at Codexis revealed that 16 KRED variants have been derived from the short-chain dehydrogenase of the bacterium *Lactobacillus kefir* (LKADH)²⁴. In the absence of mutations, LKADH can reduce 'small-bulky' substrates, such as acetophenone, but is incapable of reducing 'bulky-bulky' ketones, such as hexanophenone (Supplementary Fig. 1). However, upon mutation of tyrosine 190, LKADH gains the ability to reduce more sterically demanding substrates^{25,26}. G. Huisman revealed that the 10 most active of his 16 KRED variants contain a mutation at position tyrosine 190. Capitalizing on this information, we conducted site-saturation mutagenesis at tyrosine 190 of LKADH, and found that mutation of this amino acid to cysteine did indeed activate the protein for dehalogenation activity, albeit with low product yield (Table 1, entries 7, 8). When we also mutated amino acids that line the enzyme's active site, we discovered a variant (in which glutamic acid 145 was changed to phenylalanine, phenylalanine 147 was changed to leucine, and tyrosine 190 was changed to cysteine) that provided the dehalogenated product at a yield of 72% and an e.r. of 96/4 (Table 1, entry 9).

We hypothesize that these three latter mutations might result in a larger active site. Therefore, wild-type KREDs with naturally large active sites might also be capable of effecting the desired dehalogenation activity. We thus selected short-chain dehydrogenases with large

active sites from the bacteria *Sphingomonas yanoikuyae* (SYADH) and *Ralstonia* species (RasADH)²⁷. While SYADH provided product with a yield of only 5% and an e.r. of 63/37, RasADH was highly effective, providing lactone (**2**) with a yield of 51% and an e.r. of 92.5/7.5, favouring the (*S*)-enantiomer (Table 1, entry 11). We modelled lactone (**2**) into the crystal structure of RasADH (Protein DataBank entry 4BMS) to better understand how substrate binding occurs²⁸. In this model, interactions between the carbonyl oxygen and the side chains of tyrosine 150 and serine 137 are observed, consistent with the known mode of binding for ketones²⁹. Furthermore, the distance between the C4 of NADPH and the α -position of the lactone is reasonable for hydrogen-atom transfer (Extended Data Fig. 6).

With effective enzymes identified, we explored the scope and limitations of this method (Fig. 2). In general, RasADH provided lower yields than KRED-12 or KRED-3, presumably because of the decreased stability of RasADH compared with LKADH. Using bromolactone (**1**) or chlorolactone (**1'**) as the starting halolactone produced similar yields and selectivities (Extended Data Fig. 7). Fluoro- or chloro-substituted lactones provided product in high yields and excellent enantioselectivity (Fig. 2, compounds **5**, **7**). In the case of bromolactone (**9**), decreased conversions were observed owing to poor substrate solubility (Fig. 2, compound **9**). *Ortho*-substituents were well tolerated, providing product in good yield and excellent enantioselectivity (Fig. 2, compound **11**). Interestingly, lactones with decreased redox potentials were viable substrates, providing product in good yields and enantioselectivity (Fig. 2, compounds **15**, **21**). Additional stereocentres were tolerated, providing product with excellent selectivity for the *trans*-isomer (Fig. 2, compound **13**). γ -Lactones were also effective substrates, but required

KRED-3 to achieve good levels of enantioselectivity (Fig. 2, compounds **17**, **19** and **21**).

We also carried out mechanistic experiments to further elucidate the nuances of this reaction. When the reaction is run with deuterated (D_8) isopropyl alcohol, such that deuterated NAD(P)H is generated *in situ*, deuterolactone (**22**) is formed predominantly (92% deuterium incorporation), with excellent enantioselectivity (e.r. = 98/2), supporting nicotinamide's role as the hydrogen-atom source. (Fig. 3a and Supplementary Fig. 10). Over the course of the reaction, racemic halolactones are converted to enantioenriched product. Although the radical species is prochiral, it is unlikely that it survives for long enough to diffuse into the enzyme's active site. As such, we were curious as to whether a kinetic resolution of the starting material occurs over the course of the reaction. Surprisingly, there appears to be very little preference for one enantiomer of starting material over the other (Fig. 3b). To confirm this hypothesis, we reduced the structurally related ketone (**23**) using KRED-12 (Fig. 3c). The resulting alcohols (**24** and **25**) were isolated with a 50% yield of each diastereomer, with an e.r. of 96/4 and 99/1, respectively, with respect to the alcohol stereocentre. In both cases, the alcohol stereocentre was formed selectively as the (*R*)-isomer, matching the observed selectivity in the dehalogenation reaction. These results suggest that KRED-12 cannot distinguish between enantiomers at the α -position of lactones and cyclic ketones³⁰. Indeed, docking models indicate that RasADH can bind both enantiomers of the starting material (Supplementary Fig. 2).

On the basis of these findings, we propose the mechanism outlined in Fig. 3d. Irradiation of the charge-transfer complex, which comprises halolactone (**1**) and NAD(P)H within the active site of KRED (**I**), effects an electron transfer to form $I^{\bullet-} \cdot NADPH^+ \subset KRED$ (**II**, where \subset symbolizes inclusion in the active site). This, upon mesolytic cleavage of the C–Br bond, forms $I^{\bullet} \cdot NADPH^+ \subset KRED$ (**III**). We hypothesize that both enantiomers of starting material bind within the active site and, upon dehalogenation and formation of prochiral radical I^{\bullet} , undergo a conformational change within the active site for the enantio-determining hydrogen-atom transfer, to form $2 \cdot NADPH^+ \subset KRED$ (**IV**). Finally, $NADPH^+$ can be reduced by either isopropyl alcohol (using native alcohol dehydrogenase activity) or glucose dehydrogenase to complete the catalytic cycle.

In conclusion, we have found that photoexcitation of nicotinamide-dependent enzymes can cause them to become catalytically promiscuous. We anticipate that this strategy will enable many radical-mediated reactions to be rendered highly selective.

Online Content Methods, along with any additional Extended Data display items and Source Data, are available in the online version of the paper; references unique to these sections appear only in the online paper.

Data Availability The data that support the findings in this study are available from the corresponding author upon reasonable request.

Received 17 May; accepted 14 October 2016.

- Bornscheuer, U. T. *et al.* Engineering the third wave of biocatalysis. *Nature* **485**, 185–194 (2012).
- Bornscheuer, U. T. & Kazlauskas, R. J. in *Enzyme Catalysis in Organic Synthesis*, Ch. 41 (eds Drauz, K., Gröger, H. & May, O.) 1695–1723 (Wiley VCH, 2012).
- Prier, C. K. & Arnold, F. H. Chemomimetic biocatalysis: exploiting the synthetic potential of cofactor-dependent enzymes to create new catalysts. *J. Am. Chem. Soc.* **137**, 13992–14006 (2015).
- Blumenstein, M., Schwarzkopf, K. & Metzger, J. O. Enantioselective hydrogen transfer from a chiral tin hydride to a prochiral carbon-centered radical. *Angew. Chem. Int. Edn* **36**, 235–236 (1997).
- Zimmerman, J. & Sibi, M. P. Enantioselective radical reactions. *Top. Curr. Chem.* **263**, 107–162 (2006).
- Meggers, E. Asymmetric catalysis activated by visible light. *Chem. Commun. (Camb.)* **51**, 3290–3301 (2015).
- Frey, P. A. Radical mechanisms of enzymatic catalysis. *Annu. Rev. Biochem.* **70**, 121–148 (2001).
- Maciá-Agulló, J. A., Corma, A. & Garcia, H. Photobiocatalysis: the power of combining photocatalysis and enzymes. *Chemistry* **21**, 10940–10959 (2015).
- Park, J. H. *et al.* Cofactor-free light-driven whole-cell cytochrome P450 catalysis. *Angew. Chem. Int. Edn* **54**, 969–973 (2015).

- Conrad, K. S., Manahan, C. C. & Crane, B. R. Photochemistry of flavoprotein light sensors. *Nat. Chem. Biol.* **10**, 801–809 (2014).
- Gabruk, M. & Mysliak-Kurczel, B. Light-dependent protochlorophyllide oxidoreductase: phylogeny, regulation, and catalytic properties. *Biochemistry* **54**, 5255–5262 (2015).
- Prier, C. K., Rankic, D. R. & MacMillan, D. W. C. Visible light photoredox catalysis with transition metal complexes: applications in organic synthesis. *Chem. Rev.* **113**, 5322–5363 (2013).
- Gu, Y., Ellis-Guardiola, K., Srivastava, P. & Lewis, J. C. Preparation, characterization, and oxygenase activity of a photocatalytic artificial enzyme. *ChemBioChem* **16**, 1880–1883 (2015).
- Fukuzumi, S., Hironaka, K. & Tanaka, T. Photoreduction of alkyl halides by an NADH model compound. an electron transfer chain mechanism. *J. Am. Chem. Soc.* **105**, 4722–4727 (1983).
- Fukuzumi, S., Inada, S. & Suenobu, T. Photoinduced mechanisms of electron-transfer oxidation of NADH analogues and chemiluminescence. Detection of the keto and enol radical cations. *J. Am. Chem. Soc.* **125**, 4808–4816 (2003).
- Jung, J., Kim, J., Park, G., You, Y. & Cho, E. J. Selective debromination and α -hydroxylation of α -bromo ketones using Hantzsch esters as photoreductants. *Adv. Synth. Catal.* **358**, 74–80 (2016).
- Xu, H.-J., Liu, Y.-C., Fu, Y. & Wu, Y.-D. Catalytic hydrogenation of α,β -epoxy ketones to form β -hydroxyketones mediated by an NADH coenzyme model. *Org. Lett.* **8**, 3449–3451 (2006).
- Zhu, X.-Q. *et al.* Determination of the C4-H bond dissociation energies of NADH models and their radical cations in acetonitrile. *Chemistry* **9**, 871–880 (2003).
- Narayanan, J. M. R., Tucker, J. W. & Stephenson, C. R. J. Electron-transfer photoredox catalysis: development of a tin-free reductive dehalogenation reaction. *J. Am. Chem. Soc.* **131**, 8756–8757 (2009).
- Maidan, R. & Willner, I. Photochemical and chemical enzyme catalyzed debromination of meso-1,2-dibromostilbene in multiphase systems. *J. Am. Chem. Soc.* **108**, 1080–1082 (1986).
- Huisman, G. W., Liang, J. & Krebber, A. Practical chiral alcohol manufacture using ketoreductases. *Curr. Opin. Chem. Biol.* **14**, 1–8 (2009).
- Kara, S. *et al.* Access to lactone building blocks via horse liver alcohol dehydrogenase-catalyzed oxidative lactonization. *ACS Catal.* **3**, 2436–2439 (2013).
- Kao, T.-H., Chen, Y., Pai, C.-H., Chang, M.-C. & Wang, A. H.-J. Structure of a NADPH-dependent blue fluorescent protein revealed the unique role of Gly176 on the fluorescence enhancement. *J. Struct. Biol.* **174**, 485–493 (2011).
- Hummel, W. Reduction of acetophenone to *R*(+)-phenylethanol by a new alcohol dehydrogenase from *Lactobacillus kefir*. *Appl. Microbiol. Biotechnol.* **34**, 15–19 (1990).
- Noey, E. L. *et al.* Origins of stereoselectivity in evolved ketoreductases. *Proc. Natl Acad. Sci. USA* **112**, E7065–E7072 (2015).
- Niefind, K., Müller, J., Riebel, B., Hummel, W. & Schomburg, D. The crystal structure of R-specific alcohol dehydrogenase from *Lactobacillus brevis* suggests the structural basis of its metal dependency. *J. Mol. Biol.* **327**, 317–328 (2003).
- Man, H. *et al.* Structures of alcohol dehydrogenases from *Ralstonia* and *Sphingobium* spp. reveal the molecular basis for their recognition of 'bulky-bulky' ketones. *Top. Catal.* **57**, 356–365 (2014).
- Trott, O. & Olson, A. J. AutoDock Vina: improving the speed and accuracy of docking with a new scoring function, efficient optimization and multithreading. *J. Comput. Chem.* **31**, 455–461 (2010).
- Sanli, G., Dudley, J. I. & Blaber, M. Structural biology of the aldo-keto reductase family of enzymes: catalysis and cofactor binding. *Cell Biochem. Biophys.* **38**, 79–101 (2003).
- Cuetos, A. *et al.* Access to enantiopure α -alkyl- β -hydroxy esters through dynamic kinetic resolutions employing purified/overexpressed alcohol dehydrogenases. *Adv. Synth. Catal.* **354**, 1743–1749 (2012).

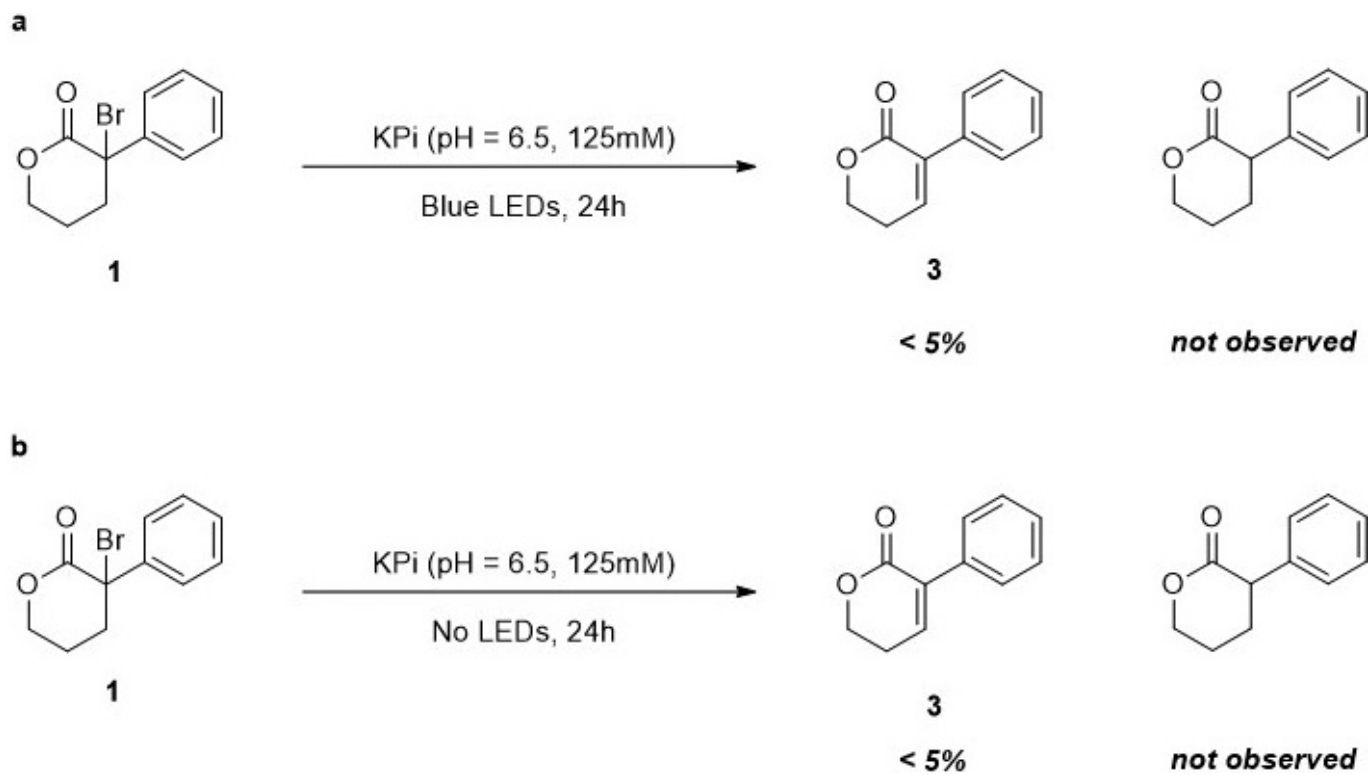
Supplementary Information is available in the online version of the paper.

Acknowledgements Financial support was provided by Princeton University. D.G.O. also acknowledges financial support from the Natural Sciences and Engineering Research Council of Canada (NSERC). We thank the MacMillan group for use of their chiral high-performance liquid-chromatography and cyclic-voltammetry equipment; G. Scholes for providing the time-resolved fluorescence instrument; H. Yayla of the Knowles group for assistance with cyclic-voltammetry experiments; B. Shields of the Doyle group and the Scholes Group for collection of the LED emission spectrum; and G. Huisman of Codexis for conversations regarding the nature of the mutants in the Codexis KRED kit.

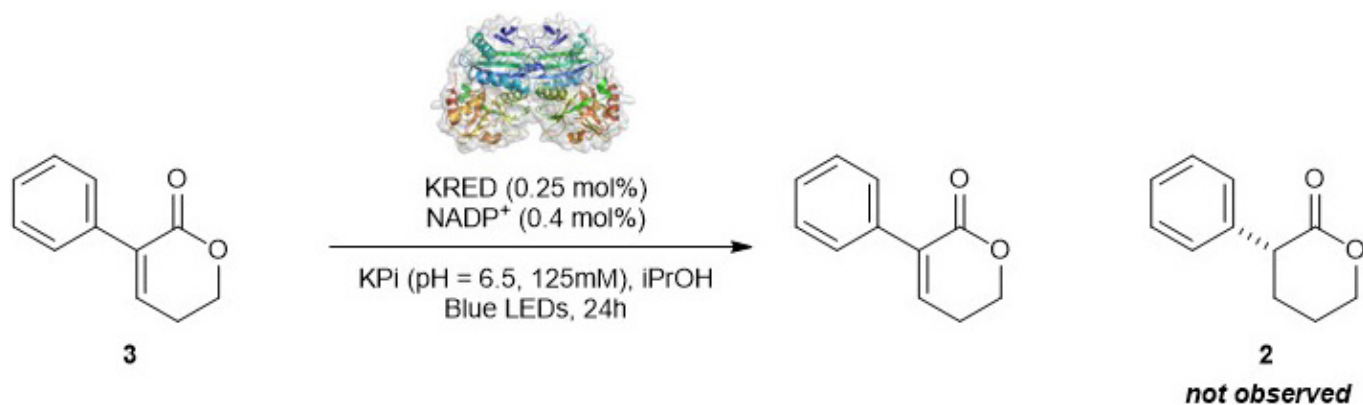
Author Contributions M.A.E and T.K.H. designed the experiments, performed and analysed experiments, and prepared the manuscript. N.R.G. performed and analysed experiments. D.G.O. collected and analysed time-resolved fluorescence data.

Author Information Reprints and permissions information is available at www.nature.com/reprints. The authors declare no competing financial interests. Readers are welcome to comment on the online version of the paper. Correspondence and requests for materials should be addressed to T.K.H. (thyster@princeton.edu).

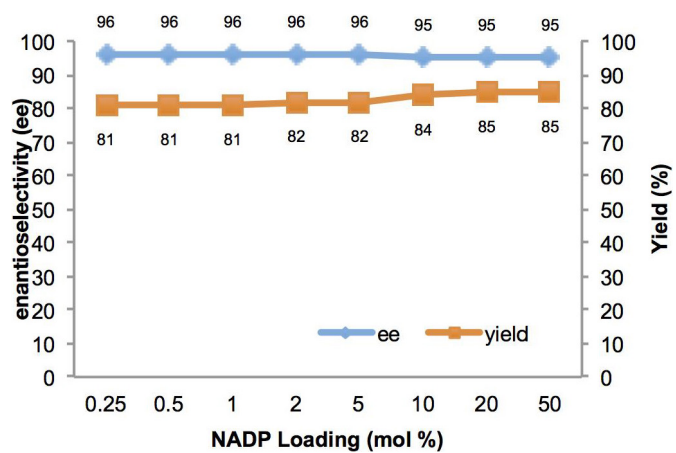
Reviewer Information *Nature* thanks E. Meggers and the other anonymous reviewer(s) for their contribution to the peer review of this work.



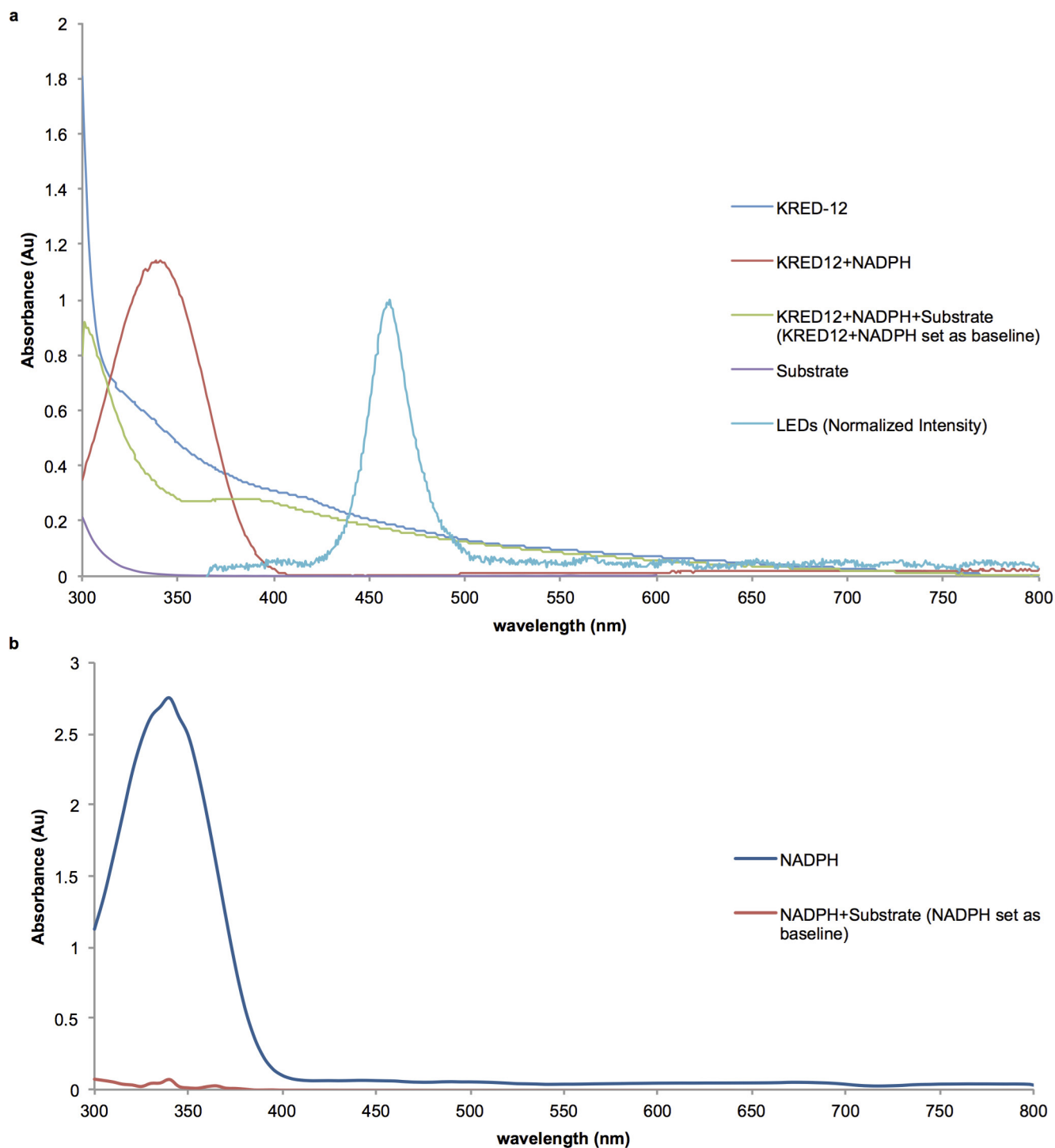
Extended Data Figure 1 | Control experiments for degree of elimination product. a, b, Lactone (**1**) does not undergo spontaneous dehydrogenation to produce dehydrolactone (**3**) in solution, either under irradiation (**a**) or without irradiation (**b**). This further suggests that the reaction is not proceeding via KRED-catalysed alkene reduction.



Extended Data Figure 2 | Control for promiscuous alkene-reductase activity. Dehydrolactone (3, left) is unreactive under our reaction conditions; thus, product 2 is not formed by KRED-catalysed alkene reduction.

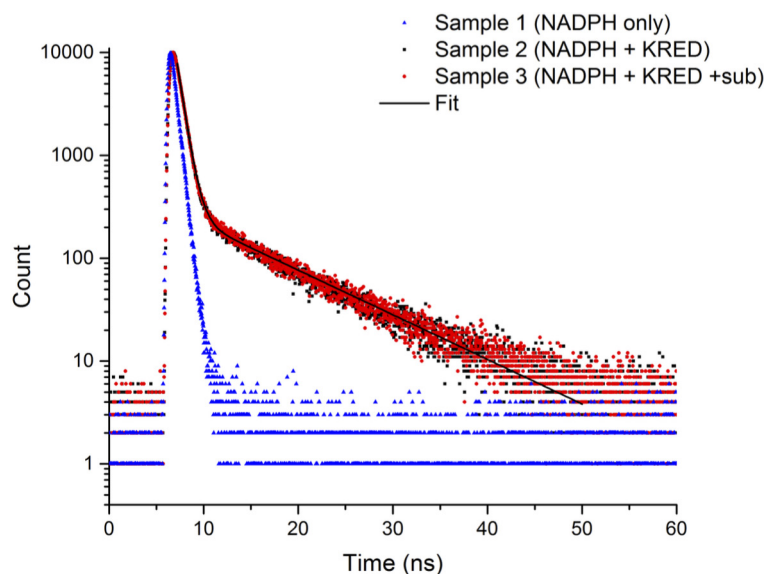


Extended Data Figure 3 | Control for the effects of excess nicotinamide. Product yield and enantiomeric excess remain relatively unchanged over a wide range of NADP loadings. This suggests that, once KRED is fully loaded with NADP, further increases in NADP concentration have little effect; that is, NADP needs to be bound to KRED in order to exert its effect in this reaction.



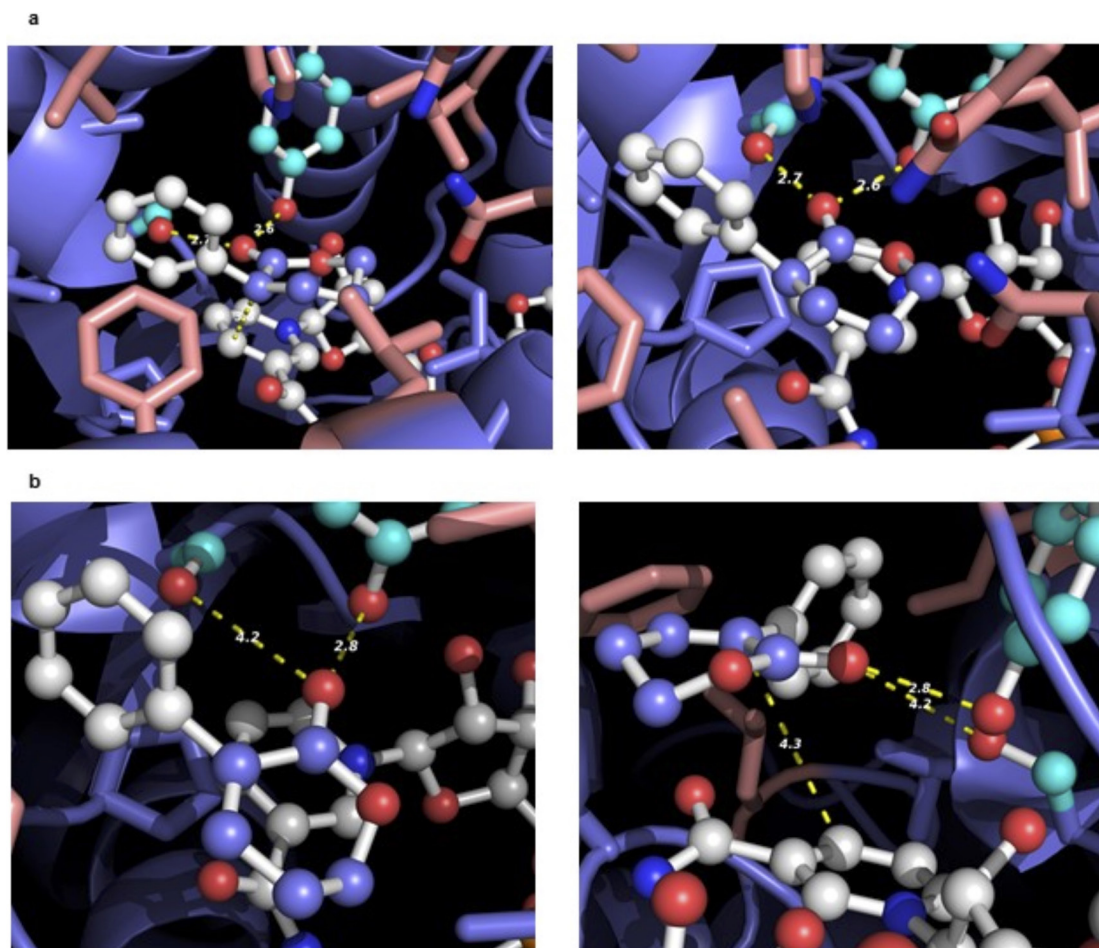
Extended Data Figure 4 | Absorbance spectra. a, In the presence of KRED, there is a redshift in the absorbance spectrum of NADPH when substrate is added to the system. This shift is potentially indicative of a charge-transfer complex being formed between the substrate and NADPH. These spectra are overlaid with the emission spectrum of the

blue LED source used in all experiments. **b**, In the absence of KRED, no such absorption shift is seen when substrate is added. Together, these data suggest that light (LED) irradiates a charge-transfer complex comprising substrate, NADPH and enzyme to initiate the catalytic cycle.

**Extended Data Figure 5 | Time-correlated single-photon counting.**

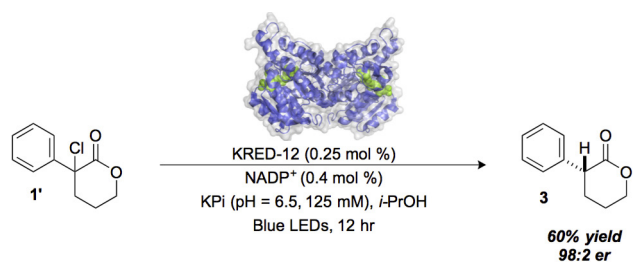
The lifetimes of fluorescence-excited states of NADPH, with and without enzyme and substrate, were determined using time-correlated single-photon counting (TCSPC) on a HORIBA Scientific DeltaFlex TCSPC system. Each sample was concentrated to an optical density of

approximately 0.1 absorbance units and excited using a 305-nm laser; fluorescence emission decay was then probed at 460 nm. Data analysis was done using HORIBA Scientific DAS6 decay analysis software, whereby each data set was fit to an exponential curve to obtain the lifetimes.



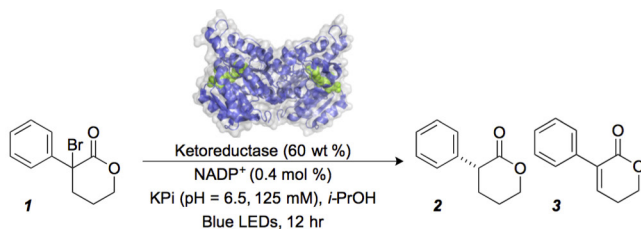
Extended Data Figure 6 | Docking models. Automated docking models were obtained using Autodock Vina²⁸. Panels **a** and **b** indicate two different docking poses as predicted by Autodock. Chain C of RasADH (PDB = 4BMS) was used as a receptor and prepared using Autodock tools. Coordinates for all ligands were prepared using Gaussian and Autodock tools. The active site of RasADH was contained in a $10 \times 10 \times 10$ grid with 1 Å spacing, centred around position $45 \times 9.431 \times 37.226$, which approximately corresponds to the C4–H bond of NADPH.

The exhaustiveness parameter was set to 10 and the rest of the docking parameters were set to default. Docking models for substrate **2** were accessed for their ability to rationalize the observed stereochemistry and provide a reasonable distance and geometry for hydrogen-atom transfer. The blue ribbon shows chain C of RasADH. Substrate **2** is shown in ball-and-stick format, with oxygens in red, lactone carbons in blue, and aromatic carbons in white. The left and right images are two different views of the same model.



Extended Data Figure 7 | Chlorolactone 1' in dehalogenation. The halolactone **1'** shows similar reactivity to its bromolactone counterpart (**1**) under the same reaction conditions.

Extended Data Table 1 | Screen of commercially available KREDs



Abbreviation	Ketoreductase Variant	Parent ADH	Mutation to Y190	er 2	Yield (%) 2	Yield (%) 3
KRED-1	KRED-P1A04	<i>L. kefir</i>	No	-	8	20
KRED-2	KRED-P1A12	<i>L. kefir</i>	No	-	9	20
KRED-3	KRED-P1B02	<i>L. kefir</i>	Yes	97:3	34	14
KRED-4	KRED-P1B05	<i>L. kefir</i>	Yes	98:2	81	5
KRED-5	KRED-P1B10	<i>L. kefir</i>	Yes	85:15	34	15
KRED-6	KRED-P1B12	<i>L. kefir</i>	Yes	90:10	20	13
KRED-7	KRED-P1C01	<i>L. kefir</i>	Yes	93:7	67	17
KRED-8	KRED-P1H08	<i>L. kefir</i>	No	-	6	15
KRED-9	KRED-P2B02	<i>L. kefir</i>	Yes	97:3	50	8
KRED-10	KRED-P2C02	<i>L. kefir</i>	Yes	93:7	35	8
KRED-11	KRED-P2C11	<i>L. kefir</i>	No	-	7	41
KRED-12	KRED-P2D03	<i>L. kefir</i>	Yes	98:2	81	4
KRED-13	KRED-P2D11	<i>L. kefir</i>	Yes	86:14	25	16
KRED-14	KRED-P2D12	<i>L. kefir</i>	Yes	98:2	81	5
KRED-15	KRED-P2G03	<i>L. kefir</i>	No	-	11	27
KRED-16	KRED-P2H07	<i>L. kefir</i>	No	-	7	25
KRED-17	KRED-P3B03	<i>Thermobacter b.</i>	-	-	7	25
KRED-18	KRED-P3G09	<i>Thermobacter b.</i>	-	-	7	25
KRED-19	KRED-P3H12	<i>Thermobacter b.</i>	-	-	6	24
KRED-20	KRED-134	<i>wild type</i>	-	-	12	23

Reaction results obtained using 20 genetically different KREDs (purchased from Codexis).

Extended Data Table 2 | Time-correlated single-photon counting

Sample	Curve	T1 (s)	T2 (s)	
1	NADPH only	Monoexponential	$4.05 \times 10^{-10} \pm 0.026$	-
2	NADPH with KRED	Biexponential	$3.85 \times 10^{-10} \pm 0.125$	$7.92 \times 10^{-2} \pm 1.7$
3	NADPH with KRED and substrate	Biexponential	$4.00 \times 10^{-10} \pm 0.05$	$9.00 \times 10^{-2} \pm 0.12$
4	KRED only	N/A	N/A	N/A
5	Substrate only	N/A	N/A	N/A

Time-correlated single-photon fluorescence decays for NADPH, NADPH plus KRED, and NADPH plus KRED plus substrate. T1 and T2 are the lifetimes of fitted exponential fluorescence decay kinetics. The fluorescence lifetimes obtained for only NADPH are consistent with literature values²³. Samples 2 and 3 produce biexponential curves, indicating the presence of two distinct fluorescent species. Considering the similarities among all T1 values, we determine the fluorescent species to be free NADPH and KRED-bound NADPH. No fluorescence was observed in enzyme-only or substrate-only controls.

have a three-dimensional lining made up of amino-acid side chains from helices 1, 2, 3, 6 and 7. These similarities indicate that the allosteric pocket might be present in other chemokine receptors. If this supposition holds true, medicinal and computational chemists will have a field day using structure-aided design strategies to develop drugs that target the pocket. Vercirnon, for example, was not optimized for the CCR9 pocket, and it is likely that some minor alterations would improve its drug properties.

The structures also provide insights into the mechanism of intracellular allosteric antagonism. Both show that the bound antagonists prevent outward movement and rotation of helices (especially helix 6), which is the hallmark of the active-state structure. Particularly in the CCR9-vercirnon structure, in which the cytoplasmic loops are not modified for crystallization and are reasonably well resolved, it is clear that vercirnon occupies a space that would normally be filled by the carboxy-terminal tail of a bound G protein during receptor activation⁸. Binding by the protein β -arrestin, which inhibits signalling and causes receptors to be internalized into the cell, would also certainly clash with bound vercirnon⁹.

Although structures have been produced for the human chemokine receptor CXCR4 in complex with a chemokine from a virus¹⁰, and for a viral chemokine receptor in complex with the human chemokine CX3CL1 (ref. 7), there is not yet a structure of a human chemokine receptor in complex with a human chemokine. Chemokines themselves are relatively complex protein ligands, generally comprising about 70 amino acids. What is clear is that multiple regions of the extracellular surface of chemokine receptors have roles in docking the chemokine before it can engage the orthosteric pocket in the helix bundle¹¹. Identification of a cytoplasmic allosteric binding pocket in chemokine receptors is especially valuable, because it provides an alternative strategy for structure-based drug discovery before the precise binding mode of chemokines has been fully elucidated.

Progress in developing useful small-molecule drugs for chemokine receptors has been slow. There have been just two successes — maraviroc, which targets CCR5 to prevent HIV-1 from entering cells, and plerixafor, which targets CXCR4 to mobilize bone-marrow stem cells for transplantation in people with cancer. Another dozen or so chemokine receptors are drug targets for diseases ranging from autoimmune disorders to cancer metastasis. The intracellular binding pocket identified in the current studies might provide a new strategy for inhibiting these receptors, by turning drug-discovery efforts inside out. ■

Thomas P. Sakmar and Thomas Huber
are in the Laboratory of Chemical Biology

and Signal Transduction, The Rockefeller University, New York, New York 10065, USA.
e-mails: sakmar@rockefeller.edu;
hubert@rockefeller.edu

- Oswald, C. *et al. Nature* **540**, 462–465 (2016).
- Zheng, Y. *et al. Nature* **540**, 458–461 (2016).
- De Lean, A., Stadel, J. M. & Lefkowitz, R. J. *J. Biol. Chem.* **255**, 7108–7117 (1980).
- Zweemer, A. J. M. *et al. Mol. Pharmacol.* **84**, 551–561 (2013).
- Tchernychev, B. *et al. Proc. Natl Acad. Sci. USA* **107**,

- 22255–22259 (2010).
- Staus, D. P. *et al. Nature* **535**, 448–452 (2016).
- Burg, J. S. *et al. Science* **347**, 1113–1117 (2015).
- Rasmussen, S. G. F. *et al. Nature* **477**, 549–555 (2011).
- Kang, T. *et al. Nature* **523**, 561–567 (2015).
- Qin, L. *et al. Science* **347**, 1117–1122 (2015).
- Veldkamp, C. T. *et al. Sci. Signal.* **1**, ra4 (2008).
- Tan, Q. *et al. Science* **341**, 1387–1390 (2013).

This article was published online on 7 December 2016.

CHEMICAL BIOLOGY

A radical change in enzyme catalysis

A method has been devised that allows a ketoreductase enzyme to catalyse reactions other than its natural ones. The key is to excite the enzyme's cofactor using light — an approach that might work for other enzymes. SEE LETTER P.414

UWE T. BORNSCHEUER

Enzymes have several advantages over conventional catalysts for organic synthesis. For example, their ability to perform reactions at room temperature in water makes them suitable for environmentally friendly chemical processes. But many synthetically useful reactions cannot be catalysed by naturally occurring enzymes. The quest to expand nature's enzymatic repertoire of transformations is therefore a crucial area of research. On page 414, Emmanuel *et al.*¹ report a strategy that allows ketoreductase enzymes to perform completely different reactions from the ones that they evolved to catalyse.

Living organisms are without doubt the best chemists on Earth — a plethora of reaction types is catalysed by the thousands of different enzymes present in every cell. The reactions take place with excellent selectivity (forming solely the desired product), astonishing efficiency (performing hundreds of catalytic reactions per second at a single catalytic site) and at ambient temperatures and pH values. By contrast, chemists have developed methods that allow a range of reactions with no enzymatic counterpart to be easily performed. In many cases, developing an enzyme that can perform such reactions is desirable.

Researchers have therefore devised a range of concepts for creating or modifying proteins to catalyse reactions unknown in nature^{2–4}. One approach is to incorporate chemical transition-metal catalysts into protein scaffolds. As early as 1978, the protein avidin was modified to incorporate a rhodium catalyst⁵, producing an enzyme that catalyses asymmetric hydrogenations — transformations in which hydrogen reacts

with organic molecules to produce products predominantly as one mirror-image isomer (enantiomer). This year, a system in which a ruthenium catalyst was incorporated into the streptavidin protein enabled olefin metathesis (a carbon–carbon bond-formation reaction; Fig. 1a) *in vivo* in the bacterium *Escherichia coli*⁶.

A second general approach is to use protein engineering to redesign enzymes to catalyse reactions other than the native one. This strategy is exemplified by the engineering of P450 monooxygenase enzymes⁷ to catalyse carbon–carbon bond-formation reactions (cyclopropanations; Fig. 1b), rather than the analogous carbon–oxygen bond-formation reactions (epoxidations) that occur naturally. A third approach is computational *de novo* protein design, which has been used to make an enzyme that catalyses the Kemp elimination reaction, in which a hydrogen ion (H⁺) is removed from a carbon atom in an organic molecule (Fig. 1c)⁸. Subsequent extensive protein engineering through directed evolution of the enzyme resulted in catalytically efficient mutants⁹.

Emmanuel *et al.* now report a striking new concept for generating enzymes that catalyse unnatural reactions: the authors use light to excite a cofactor (NAD(P)H) bound in the active site of a ketoreductase (KRED) enzyme. The resulting photoexcited cofactor generates a radical intermediate that serves as a hydrogen source. Furthermore, this hydrogen source is chiral — it has a 'handedness' that can potentially be passed on to other molecules during reactions. The authors find that, when KRED contains a photoexcited cofactor, it catalyses a reaction in which a halogen atom is removed from molecules known as halolactones,

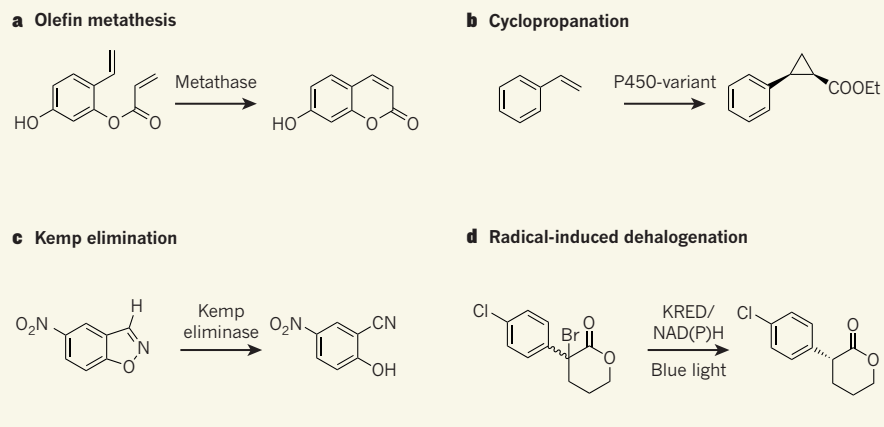


Figure 1 | Non-natural reactions catalysed by enzymes. Several strategies have been devised to develop enzymes that catalyse reactions unknown in nature. **a**, Synthetic catalysts can be incorporated into naturally occurring proteins. This approach was used to prepare metathase enzymes that catalyse olefin metathesis⁶. **b**, Enzymes can be engineered to catalyse non-natural reactions — for example, P450 enzymes have been engineered to promote the cyclopropanation reaction⁷. **c**, Kemp eliminase enzymes have been designed *de novo* computationally⁸, to perform the Kemp elimination reaction. **d**, Emmanuel *et al.*¹ now report that the cofactor NAD(P)H can be excited by blue light in ketoreductase (KRED) enzymes. This enables the enzyme to catalyse an unnatural reaction known as radical-induced dehalogenation, which yields the product as predominantly one mirror-image isomer (enantiomer). Et, ethyl; Cl, chlorine; Br, bromine.

forming products predominantly as one enantiomer (Fig. 1d). Moreover, the enantiomer that is formed depends on the preference of the KRED that is used. The authors show that this unnatural reaction can be used to generate either of the enantiomers of products formed from a broad range of halolactones, demonstrating the synthetic usefulness of this approach.

The KRED fulfils two functions in this reaction. First, it ensures productive, coordinated binding of the photoexcited NAD(P)H with the halolactone in its active site. But it also recycles the spent cofactor by reacting it with isopropanol (a component of the reaction mixture), regenerating NAD(P)H. This efficient recycling enables a KRED molecule to mediate multiple catalytic cycles, as would be needed for the enzyme to be used to make gram or kilogram quantities of product for industrial applications.

Not all the KREDs investigated by the authors could catalyse the reaction; Emmanuel and colleagues found that certain point mutations in the enzyme are needed to promote the productive binding of NAD(P)H within the enzyme's scaffold. However, the catalytically active KREDs bind the halolactones perfectly, even though they do not resemble the enzymes' natural substrates. Furthermore, the authors proved that the unnatural reaction occurs only when NAD(P)H is tightly bound to KRED and is irradiated with blue light.

The authors proposed a mechanism for the reaction in which light irradiation causes an electron to be transferred between the NAD(P)H and the substrate, triggering cleavage of the substrate's carbon–halogen bond,

and thus generating a radical intermediate that accepts a hydrogen atom to form the final product enantioselectively (see Fig. 3d of the paper¹). They nicely confirm this mechanism by generating a deuterium donor from NAD(P)H *in situ* in KRED, and observing where the deuterium is incorporated into the reaction products.

Emmanuel *et al.* have demonstrated a completely new strategy for accessing

unnatural enzymatic reactions by exploring the interface between photochemistry and protein science. Other synthetic transformations can be envisaged with this approach, by using light-induced changes in NAD(P)H analogues or other cofactors. For instance, the well-studied flavin cofactors (flavin adenine dinucleotide, flavin mononucleotide and their artificial analogues) could be prime candidates for investigation, because various flavin-dependent enzymes are important biological catalysts used by synthetic chemists¹⁰. In combination with modern tools for protein engineering¹¹, the authors' concept is likely to have a strong impact on the use of various enzyme classes in biocatalysis. ■

Uwe T. Bornscheuer is in the Department of Biotechnology and Enzyme Catalysis, Institute of Biochemistry, Greifswald University, 17489 Greifswald, Germany.

e-mail: uwe.bornscheuer@uni-greifswald.de

- Emmanuel, M. A., Greenberg, N. R., Oblinsky, D. G. & Hyster, T. K. *Nature* **540**, 414–417 (2016).
- Hyster, T. K. & Ward, T. R. *Angew. Chem. Int. Edn* **55**, 7344–7357 (2016).
- Renata, H., Wang, Z. J. & Arnold, F. H. *Angew. Chem. Int. Edn* **54**, 3351–3367 (2015).
- Bornscheuer, U. T. *et al. Nature* **485**, 185–194 (2012).
- Wilson, M. E. & Whitesides, G. M. *J. Am. Chem. Soc.* **100**, 306–307 (1978).
- Jeschek, M. *et al. Nature* **537**, 661–665 (2016).
- Coelho, P. S., Brustad, E. M., Kannan, A. & Arnold, F. H. *Science* **339**, 307–310 (2013).
- Röthlisberger, D. *et al. Nature* **453**, 190–195 (2008).
- Blomberg, R. *et al. Nature* **503**, 418–421 (2013).
- Toogood, H. S., Gardiner, J. M. & Scrutton, N. S. *ChemCatChem* **2**, 892–914 (2010).
- Kazlauskas, R. J. & Bornscheuer, U. T. *Nature Chem. Biol.* **5**, 526–529 (2009).

CANCER

A gene-expression profile for leukaemia

Can simple genetic risk profiles be identified for complex diseases? The development of a gene-expression profile for acute myeloid leukaemia suggests that they can, and that they may improve prognosis prediction. SEE LETTER P.433

GERRIT J. SCHUURHUIS

On page 433, Ng *et al.*¹ report a tool that improves the prediction of prognoses for people who have a form of acute leukaemia. The researchers began by identifying populations of cells that exhibit key properties — collectively known as stemness — that enable the cells to initiate and sustain leukaemia. This allowed the authors to ascertain gene-expression profiles for stemness, and to use them as the basis of a scoring system for risk. The work demonstrates how

gene-expression profiles can be used to enable reliable prognoses for complex diseases.

Acute myeloid leukaemia (AML) is characterized by the presence of a huge range of chromosomal and molecular aberrations. This means that there are many subgroups of people with AML who have widely different prognoses². These groups are known as risk groups, and are used to determine which consolidation treatment should be given following initial chemotherapy (induction therapy). For example, transplantation of stem cells from donors is an option for patients judged to be